

# Magneto-structural correlation for binuclear octahedral vanadium(IV)–oxo complexes. Synthesis, structure and magnetic properties of a $V^{IV}O^{2+}$ complex with a new ligand derived from glycine

Augusto S. Ceccato,<sup>\*a</sup> Ademir Neves,<sup>a</sup> Marcos A. de Brito,<sup>a</sup> Sueli M. Drechsel,<sup>b</sup>  
Antonio S. Mangrich,<sup>b</sup> Rüdiger Werner,<sup>c</sup> Wolfgang Haase<sup>c</sup> and Adailton J. Bortoluzzi<sup>d</sup>

<sup>a</sup> Departamento de Química, Universidade Federal de Santa Catarina, 88040-900-Florianópolis, SC, Brasil. E-mail: ceccato@qmc.ufsc.br

<sup>b</sup> Departamento de Química, Universidade Federal do Paraná, Curitiba, PR, Brasil

<sup>c</sup> Institut für Physikalische Chemie, Technische Hochschule, Darmstadt, D-6100 Darmstadt, Germany

<sup>d</sup> Departamento de Química, Universidade Federal de Santa Maria, Santa Maria, RS, Brasil

Received 7th December 1999, Accepted 24th March 2000

Published on the Web 27th April 2000

The synthesis of a new ligand,  $H_3BBAC$  (*N,N*-bis(2-hydroxybenzyl)aminoacetic acid) and its first  $V^{IV}O^{2+}$  complex,  $[Et_3NH]_2[O=V(BBAC)]_2$  (**1**), are presented in order to model the active site of vanadium transferrins. Spectroscopic (EPR, UV-VIS), magnetic properties and crystal data of **1** are discussed and a new magneto-structural correlation turns out to be relevant for binuclear RO-bridging octahedral vanadium(IV)–oxo complexes.

## Introduction

Magnetic properties of molecular compounds are important in bioinorganic chemistry when one tries to correlate them with structural parameters.<sup>1–4</sup> For some dicopper(II)  $d^9$ – $d^9$  complexes it is possible to establish a quantitative correlation between magnetic and structural data,<sup>1</sup> but for binuclear octahedral vanadium(IV)–oxo complexes such data are rare.<sup>5</sup> In the oxo-vanadium case the  $d_{xy}$  orbitals are magnetically relevant to couple the  $V^{IV}$  centers in the binuclear unit when compared to binuclear copper complexes in which the  $d_{x^2-y^2}$  are the magnetic orbitals. A recent structural study of duck ovotransferrin shows two iron(III) centers coordinated to oxygen residues from tyrosines, a carboxylic oxygen from aspartate and a guanidinium group that interacts with  $CO_3^{2-}$ .<sup>6</sup> Transferrins are also able to coordinate to other transition metal ions such as vanadium in vanadium transferrins ( $[V^{IV}(tf)]$ ),<sup>7,8</sup> therefore octahedral vanadium(IV)–oxo compounds that present oxygen (from phenolate and carboxylic) and nitrogen donor groups are important to model the coordination sphere of modified transferrin.<sup>9</sup> Furthermore,  $d^1$  ( $V(IV)$ ) systems are interesting tools for EPR studies<sup>10</sup> when correlated to other magnetic and structural studies.

## Experimental

### Syntheses

**$H_2BAC$  = *N*-(2-Hydroxybenzyl)aminoacetic acid.** To a suspension of glycine (15.0 g, 200 mmol) in 250 ml of methanol, was added  $LiOH \cdot H_2O$  (8.4 g, 210 mmol). To this solution was added under stirring 24 ml (200 mmol) of salicylaldehyde, which resulted in a yellow solid. The resulting imine was analyzed by IR spectroscopy:  $\nu(C=N)$ , 1656;  $\nu_{asym}(COO^-)$  1620;  $\nu_{sym}(COO^-)$  1394  $cm^{-1}$ . The imine was dissolved in methanol and reduced to the corresponding amine with  $NaBH_4$  (3.7 g, 100 mmol) during 15 minutes under stirring. The resulting pale yellow solution was concentrated under reduced pressure and dissolved in water. The pH was adjusted to  $\approx 6.0$  and a white

solid precipitated which was washed with  $6 \times 50$  ml of water and dried at 80 °C. Yield 64% (23 g of  $H_2BAC$ ). The precursor ligand was purified (water  $\approx 90$  °C) and presents mp  $\approx 222$ – $223$  °C. IR ( $cm^{-1}$ ):  $\nu_{asym}(COO^-)$ , 1570;  $\nu_{sym}(COO^-)$ , 1460;  $\nu(NH)NH_2^+$ , combination bands centered at 2500;  $\delta(OH)$ , 1378  $cm^{-1}$ . Elemental analysis calculated for  $C_9H_{11}NO_3$ : C, 59.96; H, 6.12; N, 7.73. Found: C, 59.53; H, 5.87; N, 7.88%.

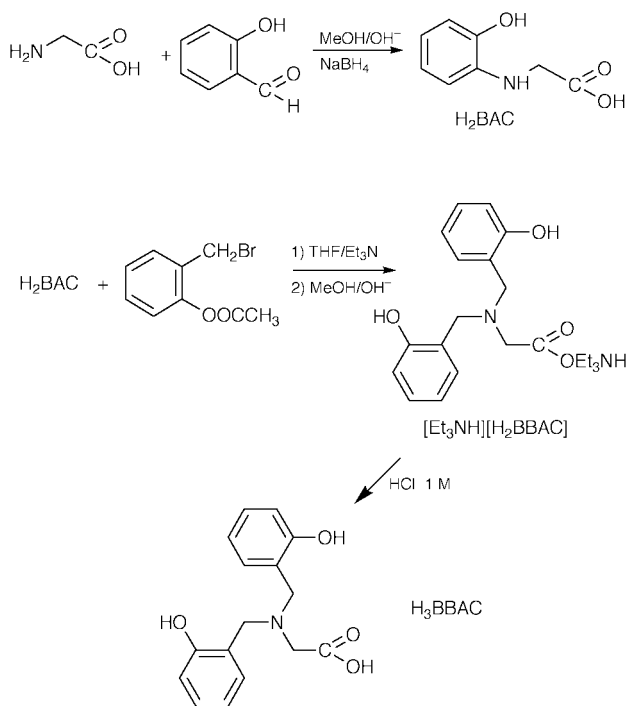
**$[Et_3NH][H_2BBAC]$  = Triethylammonium *N,N*-bis(2-hydroxybenzyl)aminoacetate.** To a solution of 2-bromomethyl phenyl acetate (11.0 g, 48 mmol) in 100 ml of THF was added  $H_2BAC$  (8.1 g, 45 mmol). To the resulting solution was added, drop by drop, 14.4 ml (105 mmol) of  $Et_3N$ , and the reaction was carried out during 24 h, under stirring. The white precipitate of  $[Et_3NH][H_2BBAC] \cdot HBr \cdot 2H_2O$  was filtered off washed with THF and diethyl ether and dried in air. Yield 21.8 g (89%), mp  $\approx 135$ – $136$  °C. IR ( $cm^{-1}$ ):  $\nu(C=O)$  ester 1768;  $\nu(NH)Et_3NH^+$  and  $NH^+ \approx 2500$  from combination bands;  $\nu(OH)PhOH$  and  $H_2O$ , 3394  $cm^{-1}$ . Elemental analysis calculated for  $C_{24}H_{38}N_2O_7Br$ : C, 52.85; H, 7.09; N, 5.14. Found: C, 53.19; H, 7.09; N, 5.35%.

The obtained ester was hydrolyzed by adding 21.8 g (40 mmol) of  $[Et_3NH][H_2BBAC] \cdot HBr \cdot 2H_2O$  to 300 ml of a methanolic solution of KOH (4.7 g, 84 mmol). The mixture was placed under stirring during 1 h, evaporated and a white solid was washed with 2-propanol ( $2 \times 50$  ml) and diethyl ether. Yield 15.6 g of  $[Et_3NH][H_2BBAC]$  that decomposes at  $\approx 255$  °C. IR ( $cm^{-1}$ ):  $\nu(OH)PhOH$ , 3358;  $\nu(NH)Et_3NH^+$ , 2600. Elemental analysis calculated for  $C_{22}H_{32}N_2O_4$ : C, 68.01; H, 8.30; N, 7.21. Found: C, 67.59; H, 7.91; N, 7.03%.

**$H_3BBAC$  = *N,N*-bis(2-hydroxybenzyl)aminoacetic acid.** The title ligand was isolated by adding HCl 1 M to 350 ml of an aqueous solution of 15.6 g of  $[Et_3NH][H_2BBAC]$  until the pH reached 4.0. A white solid was filtered off and washed 4 times with 40 ml of water and dried in the oven ( $\approx 100$  °C). Yield 6.6 g (58% relative to  $[Et_3NH][H_2BBAC] \cdot HBr \cdot 2H_2O$ ), mp  $\approx 210$ – $211$  °C. IR ( $cm^{-1}$ ):  $\nu_{asym}(COO^-)$ , 1622;  $\nu_{sym}(COO^-)$ , 1404;  $\nu(OH)$

at 2500–3000, from combination bands;  $\delta(\text{OH})$ , 1362.  $^1\text{H NMR}$  ( $\text{D}_2\text{O}$ ):  $\delta$  3.2 (2H,  $\text{CH}_2\text{OAc}$ ); 3.8 (4H,  $\text{CH}_2\text{Ar}$ ) and 6.8–7.3 (8H, ArH). No protons from OH groups were observed until 10 ppm. Elemental analysis calculated for  $\text{C}_{16}\text{H}_{17}\text{NO}_4$ : C, 66.87; H, 5.89; N, 4.88. Found: C, 66.71; H, 5.94; N, 4.74%.

Scheme 1 shows the synthetic route to obtain the title ligand.



Scheme 1

**[Et<sub>3</sub>NH]<sub>2</sub>[O=V(BBAC)]<sub>2</sub> (1).** The complex was prepared from the reaction of 0.255 g (1 mmol) of  $[\text{O}=\text{V}(\text{acac})_2]$ , dissolved in 15 ml of THF, and a solution of  $\text{H}_3\text{BBAC}$  (0.287 g, 1 mmol) and 0.83 ml (6 mmol) of  $\text{Et}_3\text{N}$  in 20 ml of THF, under argon. After 20 minutes at ambient temperature and constant stirring the green solution changed to a violet color, which was concentrated to  $\approx 6$  ml. The solution was cooled and the precipitate was filtered off and washed with acetonitrile and diethyl ether. Yield 0.28 g (31%). Elemental analysis calculated for  $\text{C}_{44}\text{H}_{60}\text{N}_4\text{O}_{10}\text{V}_2$ : C, 58.27; H, 6.67; N, 6.18. Found: C, 57.93; H, 6.59; N, 6.12%. Crystals of  $1 \cdot 4\text{CH}_2\text{Cl}_2$  suitable for single crystal X-ray analysis were obtained by slow evaporation from a dry diethyl ether/ $\text{CH}_2\text{Cl}_2$  (1:1) solution at room temperature and under an  $\text{N}_2$  atmosphere.

### Physical measurements

IR spectra were obtained on a Perkin-Elmer FTIR model I16 PC spectrometer as KBr disks. Elemental analyses were performed on a Perkin-Elmer model 2400. The  $^1\text{H NMR}$  spectrum of  $\text{H}_3\text{BBAC}$  was obtained on a Bruker 200 MHz, model AC200F in  $\text{D}_2\text{O}$ . Magnetic susceptibility data were obtained on a polycrystalline sample of  $[\text{Et}_3\text{NH}]_2[\text{O}=\text{V}(\text{BBAC})_2]$  over a temperature range from 4.5 to 300.0 K with a Faraday-type magnetometer; details of the apparatus have been described elsewhere.<sup>11</sup> Diamagnetic corrections were applied in the usual manner with the use of tabulated Pascal constants.<sup>12</sup> Visible spectra were recorded in  $\text{CH}_2\text{Cl}_2$  under argon with a Perkin-Elmer Lambda 19 spectrometer. Cyclic voltammetric experiments were performed with a PAR 273 (Princeton Applied Research) in  $\text{CH}_2\text{Cl}_2$  under argon at room temperature with 0.1 M  $[\text{Bu}_4\text{N}][\text{PF}_6]$  as the supporting electrolyte. The EPR spectrum was obtained at 77 K in X-band (9.7 GHz) on a Bruker ESP 300E spectrometer, using 100 kHz modulation frequency. The spectrum of the frozen solution was recorded using a quartz tube.

### Crystal structure determination

A violet single crystal of the  $1 \cdot 4\text{CH}_2\text{Cl}_2$  complex was isolated in inert oil, mounted on a glass fiber and quickly placed on an Enraf-Nonius CAD4 diffractometer equipped with a low temperature system. These crystals are very sensitive to solvent loss. Lattice constants were determined from 25 reflections in the  $2\theta$  range 15–27°. Cell parameter determinations and data collection were performed using CAD-4 software.<sup>13</sup> All data were corrected for Lorentz, polarization effects and for linear decay (4.1%). Empirical absorption corrections based on the azimuthal scans of 5 reflections were applied with transmission factors 0.9143–0.9999.<sup>14</sup> The structure was solved by direct methods and refined by full-matrix least-squares methods using SHELXS97<sup>15</sup> and SHELXL97<sup>16</sup> programs, respectively. All non-hydrogen atoms were refined anisotropically. An independent dichloromethane molecule was found to be disordered. Two alternative positions for each chlorine (Cl52 and Cl53) were assigned at 50% occupancy, while the carbon atom (C(51)) showed a single site occupancy. The best model for the disordered molecule was obtained by restraining C–Cl and Cl–Cl distances, isotropic and anisotropic thermal parameters. Hydrogen atoms were not located in this disordered solvent. Other hydrogens were placed at their idealized positions (C–H = 0.93 Å) with the thermal isotropic parameter fixed at 1.2 (CH,  $\text{CH}_2$ ) or 1.3 ( $\text{CH}_3$ ) times  $U_{\text{eq}}$  of the preceding atom, except for H1NA which was found from the difference Fourier map and refined as a free isotropic atom. The plot of the molecular structure of  $1 \cdot 4\text{CH}_2\text{Cl}_2$ , as shown in Fig. 1, used the program ZORTEP.<sup>17</sup> Crystal data: formula  $\text{V}_2\text{Cl}_8\text{O}_{10}\text{N}_4\text{C}_{48}\text{H}_{68}$ ;  $M = 1246.06$ ; triclinic; space group  $P\bar{1}$ ;  $a = 10.638(2)$ ;  $b = 11.380(2)$ ;  $c = 13.512(2)$  Å;  $\alpha = 98.11(3)$ ;  $\beta = 102.00(3)$ ;  $\gamma = 110.17(3)^\circ$ ;  $V = 1461.0(4)$  Å<sup>3</sup>;  $Z = 1$ ;  $T = -70^\circ\text{C}$ ;  $\mu(\text{Mo-K}\alpha) = 7.41$  cm<sup>-1</sup>; 5432 reflections collected; 5133 unique [ $R_{\text{int}} = 0.0274$ ]; final indices:  $R(F) = 0.0406$ ,  $wR(F^2) = 0.1105$  and  $\text{GOF}(F^2) = 1.066$ .

CCDC reference number 186/1911.

See <http://www.rsc.org/suppdata/dt/a9/a909846a/> for crystallographic files in .cif format.

### Results and discussion

A new tetradentate ligand,  $\text{H}_3\text{BBAC}$ , containing biologically relevant donor groups, and its first complex,  $[\text{Et}_3\text{NH}]_2[\text{O}=\text{V}(\text{BBAC})_2]$  **1** were prepared and fully characterized. The electronic spectrum of **1** in  $\text{CH}_2\text{Cl}_2$  under argon showed two d–d transitions ( $\lambda_{\text{max}}$ , 567 nm/ $\epsilon = 73$  M<sup>-1</sup> cm<sup>-1</sup> and  $\lambda_{\text{max}}$ , 787 nm/ $\epsilon = 68$  M<sup>-1</sup> cm<sup>-1</sup>). This transition changes to  $\lambda_{\text{max}}$  563 nm/ $\epsilon \approx 2100$  M<sup>-1</sup> cm<sup>-1</sup>, after 2 h when the solution has been in contact with the air, characteristic of V(v)–oxo complexes. Unfortunately we were not able to isolate the corresponding oxidation product. The reflectance spectrum of **1** (KBr pellets) showed the same transition mode when compared to the spectrum in solution. The IR spectrum of **1**, when compared to the spectrum of  $\text{H}_3\text{BBAC}$ , shows  $\nu(\text{V}=\text{O})$  at 963 cm<sup>-1</sup> that is characteristic of V(iv)–oxo compounds, and, as expected, lacks  $\delta(\text{OH})$  at 1362 cm<sup>-1</sup>. We were not able to observe any activity of the title complex on the time scale of the cyclic voltammetry experiments employed.

### Description of the molecular structure of $1 \cdot 4\text{CH}_2\text{Cl}_2$

The crystal structure of  $1 \cdot 4\text{CH}_2\text{Cl}_2$  was determined by single-crystal X-ray diffraction methods. The asymmetric unit consists of half  $[\text{O}=\text{V}(\text{BBAC})_2]^{2-}$ , a triethylammonium cation and two dichloromethane solvent molecules arranged in the space group  $P\bar{1}$ . The molecular structure of  $1 \cdot 4\text{CH}_2\text{Cl}_2$ , and selected bond lengths and angles are shown in Fig. 1.

The  $[\text{O}=\text{V}(\text{BBAC})_2]^{2-}$  unit shows a centrosymmetric structure and has two V(iv) centers bridged by two phenolate groups. The metallic ions are in pseudo-octahedral environments (Fig. 1), where O(2) of the carboxylate group occupies the *trans* position

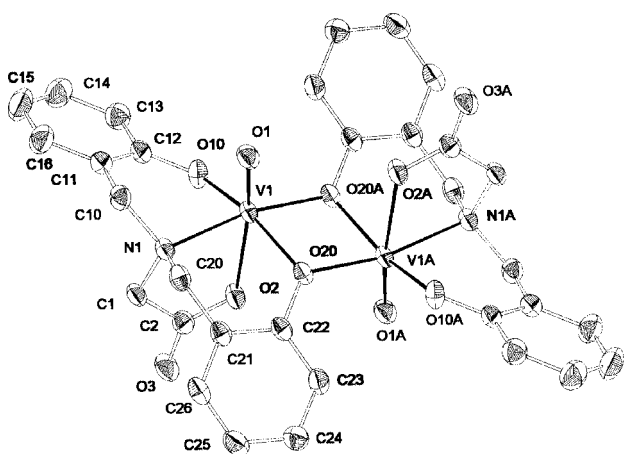


**Fig. 1** A view of the anion of  $1 \cdot 4\text{CH}_2\text{Cl}_2$  with numbering scheme. Thermal ellipsoids are shown at the 50% probability level. Hydrogen atoms are omitted for clarity. Selected bond lengths [Å] and angles [°]: V1–O1 1.610(2), V1–O10 1.948(2), V1–O20A\* 2.032(2), V1–O20 2.087(2), V1–N1 2.147(2), V1–O2 2.170(2); O1–V1–O1 99.77(8), O1–V1–O20A\* 100.85(7), O10–V1–O20A\* 95.92(7), O1–V1–O20 96.45(8), O10–V1–O20 163.77(7), O20A\*–V1–O20 81.38(7), O1–V1–N1 90.94(8), O10–V1–N1 86.11(7), O20A\*–V1–N1 167.48(7), O20–V1–N1 93.22(7), O1–V1–O2 166.44(7), O10–V1–O2 84.49(7), O20A\*–V1–O2 91.43(6), O20–V1–O2 79.60(7), N1–V1–O2 76.44(7), V1A–O20–V1 98.62(7). Symmetry operation: \*  $-x + 1, -y + 2, -z + 1$ .

with respect to the terminal oxo group. In this arrangement nitrogen and oxygen atoms from phenolates occupy equatorial positions. The terminal oxo groups are *anti* and the vanadium ion is 0.251(1) Å from the equatorial plane with respect to the terminal oxo group. The complex shows a V...V distance of 3.125, which is 0.1 Å longer than similar V–O–V complexes.<sup>13–15</sup> The V(1)–O(2) (2.170 Å) bond length is 0.12 Å shorter than the same bond observed in Na[VO(EHGS)]<sup>18</sup> (EHGS = *N*-[2-(*o*-salicylideneamino)ethyl](*o*-hydroxyphenyl)-glycine) where the carboxylate group is *trans* to the V=O group, but is 0.17 Å longer than that found in the complex NH<sub>4</sub>[VO(EHPG)],<sup>18</sup> (EHPG = ethylenebis[*o*-hydroxyphenyl]-glycine) where the carboxylate group is in the *cis* position with respect to the vanadyl group. These data indicate that the terminal oxo and carboxylate groups present a *trans* effect between them. This *trans* effect is also observed in the equatorial plane where O(20) and O(20A) are *trans* to O(10) and O(10A) from phenolates, and also with respect to N(1) and N(1A), respectively. This arrangement results in unsymmetric  $\mu$ -phenoxo bridges. The rings C(11)–C(16) and C(21)–C(26) are planar and the angle between the planes is 46.24(13)°.

## EPR

The X-band EPR powder spectrum (Fig. 2a) of **1** recorded at room temperature shows broad structured bands with peaks at 2900 and 4200 G, and a relatively low half-field absorption ( $\Delta m_S = 2$ ). This spectrum is consistent with an  $S = 1$  spin state of a dimer with low rhombicity ( $D \approx 0.1 \text{ cm}^{-1}$ ). The weak structured feature around 3400 G is attributed to a hyperfine pattern of the  $S = \frac{1}{2}$  spin state, which was also detected by the magnetic data (fit with 3.27% of paramagnetic impurity). On cooling the powder to 77 K (Fig. 2b) the strong feature of the  $S = 1$  component of the spectrum diminishes in relative intensity compared to the  $S = \frac{1}{2}$  component. The temperature dependence of the spectra is, in this case, also in agreement with the magnetic result of a  $S = 0$  ground state as expected from the results of the magnetic study which shows an antiferromagnetic coupling for the dimer. The spectrum of a freshly prepared frozen  $\text{CH}_2\text{Cl}_2$  solution of **1** (Fig. 2c), under argon atmosphere, shows the same hyperfine pattern  $S = \frac{1}{2}$  and the large signal of the  $S = 1$  component, in a similar way to the powder spectrum at 77 K. However, after five days, the spectrum of the same frozen

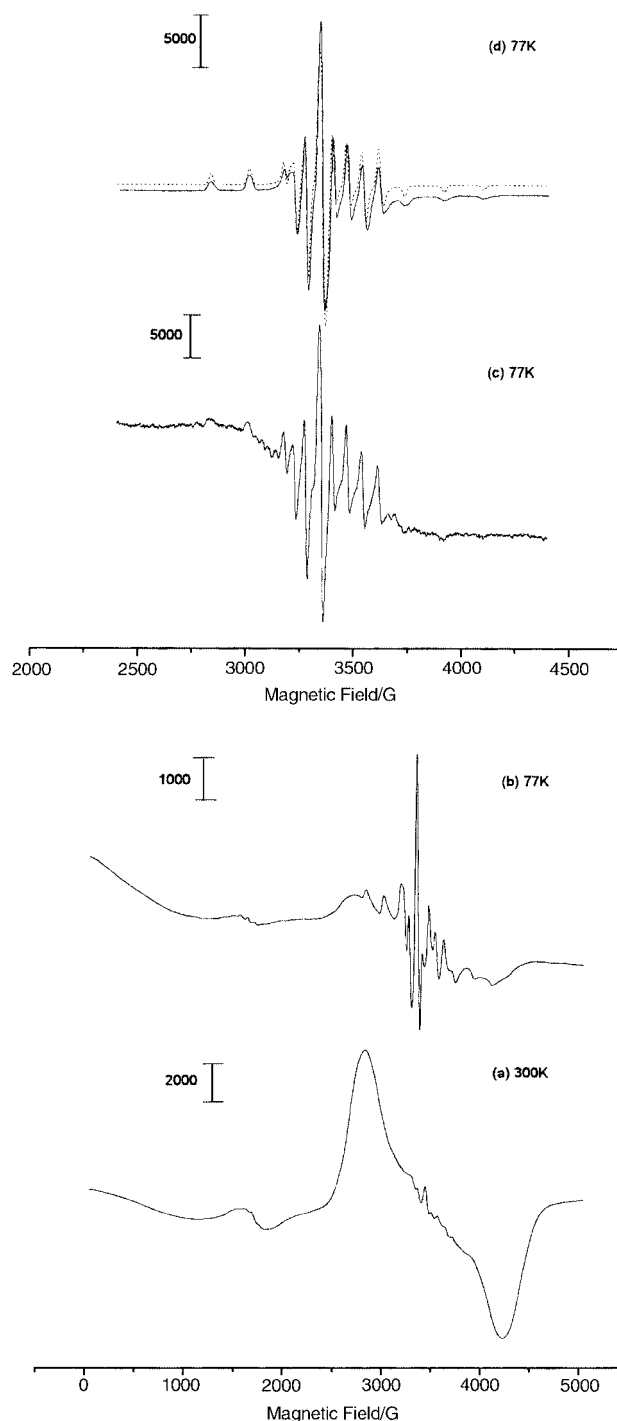


**Fig. 2** EPR powder spectra of  $[\text{O}=\text{V}(\text{BBAC})]_2^{2+}$  where (a) was recorded at 300 K and (b) at 77 K. EPR spectrum from a frozen solution in dichloromethane at 77 K (c) and (d) (— experimental, ... simulation). Simulated spectrum obtained using WINEPR SIMFONIA program.<sup>27</sup> Note the different scales.

$\text{CH}_2\text{Cl}_2$  solution of **1** (Fig. 2d) shows only the  $S = \frac{1}{2}$  component. The parameters  $g_x = 1.9750$ ,  $g_y = 1.9820$ ,  $g_z = 1.9457$  and  $A_x = 58.00$ ,  $A_y = 57.00$ ,  $A_z = 164.50$ ,  $A_{0,\text{calc.}} = 92.97 (\times 10^{-4} \text{ cm}^{-1})$  could be derived from this spectrum. From this information it seems reasonable to conclude that the structure of the dimer is not maintained in  $\text{CH}_2\text{Cl}_2$  solutions. The Hamiltonian for the solid solution is indicative of a monomeric vanadium(IV) center showing that the dimer dissociates in solution. The parameters of the monomeric species obtained in solution are similar to those of the human vanadium(IV)–transferrin ( $[\text{V}^{\text{IV}}(\text{tfh})]$ ):  $g_x = 1.973$ ,  $g_y = 1.973$ ,  $g_z = 1.938$  and  $A_x = 56.6$ ,  $A_y = 56.6$ ,  $A_z = 168$ ,  $A_{0,\text{calc.}} = 93.7 (\times 10^{-4} \text{ cm}^{-1})$ ,<sup>19</sup> where  $A_{0,\text{calc.}} = (A_x + A_y + A_z)/3$ . These data indicate that **1**, and the monomeric

**Table 1** Magnetic and structural parameters for binuclear octahedral oxovanadium(IV) compounds

Compound	$J/\text{cm}^{-1}$ ( $T/K$ )	$V \cdots V/\text{\AA}$	$V-O-V^\circ$	$\tau^\circ$	Ref.
$[\text{Et}_3\text{NH}]_2[(\text{VO})_2(\text{BBAC})_2] \cdot 4\text{CH}_2\text{Cl}_2$ ( <b>1</b> )	-167.9 (5–300)	3.125	98.6	180	This work
$[(\text{VO})_2(\text{L}^1)(\text{OCH}_3)(\text{DMSO})]^\text{a}$ ( <b>2</b> )	-122 (80–300)	3.026	94.3; 101.8	131.1	22
$[(\text{VO})_2(\text{L}^2)(\text{OH})_2]_2 \cdot 4\text{H}_2\text{O}^\text{b}$ ( <b>3</b> )	-150 (103–293)	2.965	98.1	175.7	23
$[(\text{VO})_2(\text{L}^3)(\text{OH})_2]\text{Br}_2^\text{c}$ ( <b>4</b> )	-177 (98–298)	3.033	101.2	180	24
$[(\text{VO})_2(\text{L}^4)]^\text{d}$ ( <b>5</b> )	+3.1 (4–250)	—	107.0	0.0	5

<sup>a</sup>  $\text{L}^1 = 2,6$ -Bis(salicylideneaminomethyl)-4-methylphenol. <sup>b</sup>  $\text{L}^2 = N,N,N',N'$ -Tetrakis(2-pyridylmethyl)ethylenediamine. <sup>c</sup>  $\text{L}^3 = 1,4,7$ -Triazacyclononane. <sup>d</sup>  $\text{L}^4 = N$ -Salicylidene-2-(bis(2-hydroxyethyl)amino)ethylamine.

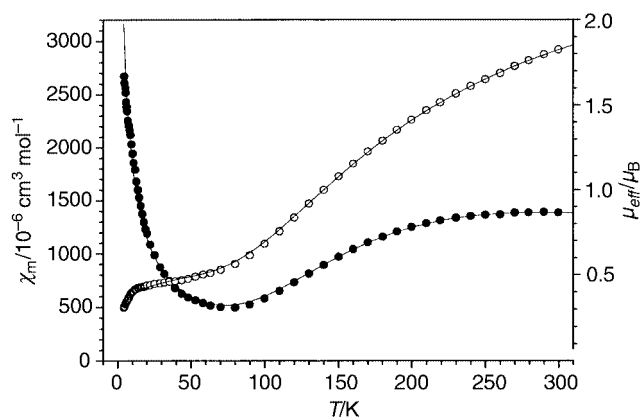


**Fig. 3** Plots of molar magnetic susceptibility per vanadium  $\chi_m$  (●) and effective magnetic moment per vanadium  $\mu_{\text{eff}}$  (○) vs. temperature for **1**.

species obtained from the dissociation of the dimer, are good models to simulate the active site structure of the enzyme. Therefore, based on the structure of the model complex, we can suggest  $\text{NO}_3$  as donor atoms in the equatorial position of the coordination sphere of the protein, where it should be possible to find two oxygen atoms from tyrosine, and a nitrogen atom from histidine.

### Magnetic properties

The variable-temperature magnetic data for complex **1** in the solid state, collected in the temperature range 4.5–300.0 K, are shown in Fig. 3 and indicate the presence of a strong antiferromagnetic coupling process.

The room temperature magnetic moment of **1** is  $1.82 \mu_B$  per binuclear molecule, which is significantly lower than the spin-only value ( $2.45 \mu_B$ ) for two uncoupled  $S = 1/2$  spins, and gradually decreases on decreasing the temperature, reaching  $0.31 \mu_B$  at 4.5 K. The data were fitted by using eqn. (1)<sup>12</sup> for

$$\chi_m = (1 - X_{\text{imp}}) \left( \frac{2Ng^2\beta^2}{kT} (3 + \exp(-J/kT))^{-1} \right) + X_{\text{imp}}(3/(8T)) + \text{TIP} = -2JS_1S_2 (S_1 = S_2 = 1/2) \quad (1)$$

molar susceptibility versus temperature derived from the spin-exchange Hamiltonian  $H$ .

For a satisfactory fit, the following parameters:  $g = 1.945$ , temperature independent magnetism (TIP) =  $83 \times 10^{-6} \text{ cm}^3 \text{ mol}^{-1}$ , paramagnetic impurity ( $X_{\text{imp}} = 3.27\%$ ),  $\theta = -3.7 \text{ K}$ ,  $J = -167.9(9) \text{ cm}^{-1}$  were used. The antiferromagnetic coupling constant of  $-167.9 \text{ cm}^{-1}$  lies in the range of values found for other binuclear vanadyl complexes containing  $\mu$ -OR bridges and dihedral angles varying between  $175.7$  to  $180^\circ$  as shown in Table 1. A more accurate analysis of the relationship between the magnetic coupling and the dihedral angle formed between the two equatorial coordination planes ( $\tau$ ) is presented in this paper. In fact, a qualitative analysis of magnetic interaction for dimers of transition metal ions could be centered at the magnetic orbitals.<sup>20</sup> In this view the electron in oxovanadium(IV)

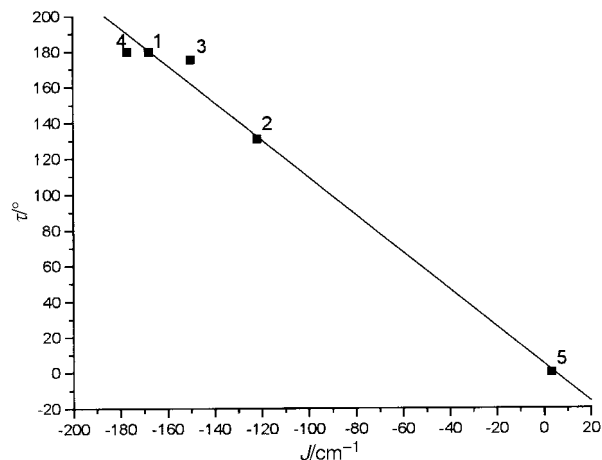


**Fig. 4** Plot of the  $J$  value vs. the dihedral angle between the equatorial planes,  $\tau$ , for binuclear RO-bridging octahedral oxovanadium(IV) complexes.

binuclear octahedral complexes generally resides in a  $d_{xy}$  orbital, with the oxo group oriented along the  $z$  direction, and this allows five magnetic interactions between the corresponding orbitals.<sup>5</sup> According to Plass<sup>5</sup> the configurations are classified in relation to the orientation of the  $V=O$  group with respect to the plane defined by the two vanadium centers and the two bridging oxygen atoms (orthogonal, coplanar and twist) and the orientation of the two  $V=O$  groups (*syn* or *anti*). From this classification there are the following possibilities: *anti*-orthogonal, *syn*-orthogonal, *anti*-coplanar, *syn*-coplanar and twist. For the orthogonal configurations a direct interaction or a superexchange mechanism between the magnetic orbitals is possible, implying a strong antiferromagnetic coupling process like those observed in complexes **1** and **4**. On the other hand for *anti*-coplanar and twist configurations<sup>5</sup> in which a direct interaction and superexchange mechanism is not effective one usually expects a ferromagnetic interaction.<sup>5,20,21</sup> We present in Table 1 magnetic data and structural parameters for binuclear RO-bridging octahedral  $V(\text{IV})$ -oxo compounds with phenoxo, alkoxo and hydroxo bridging ligands.<sup>5,22–24</sup> This series of compounds shows that  $J$  is independent of the  $V-O-V$  angle, and the  $V \cdots V$  and the  $V \cdots O$  distances. A plot of coupling constants ( $J$ ) vs. the dihedral angle ( $\tau$ ) between the two equatorial coordination planes is shown in Fig. 4.

When  $\tau$  is  $180^\circ$  (*anti*- and *syn*-orthogonal configurations respectively for complexes **1** and **4**) the interaction between the magnetic orbitals is highest and consequently the corresponding antiferromagnetic coupling is strongest. It is important to note that the *syn*-orthogonal configurations are favored in complexes **2** and **3** which exhibit steric hindrance due to the ligand and/or the number of bridges between the vanadium centers. The  $J$  values become less, relative to  $\tau$  and in the limit of  $90^\circ$  where we could expect an orthogonal situation between the magnetic orbitals, a twist<sup>5</sup> or an *anti*-coplanar configuration<sup>5,10</sup> can appear. In both cases ferromagnetic or small antiferromagnetic coupling can be detected. Therefore, Fig. 4 shows a linear dependence between the  $J$  values and  $\tau$ . Furthermore,

we can infer that  $\tau$  is the principal factor affecting  $J$  which suggests that in binuclear RO-bridging octahedral V(IV)-oxo compounds the most effective mechanism for magnetic interactions is a direct interaction between  $d_{xy}$  orbitals. Interestingly the  $[\text{HB}(\text{pz})_3\text{VO}(\text{OH})_2]_2$  complex ( $\text{HB}(\text{pz})_3$  = hydrotris(pyrazolyl)borate) shows two RO-bridges with an *anti*-orthogonal configuration ( $\tau = 180^\circ$ ) and therefore it should be strongly antiferromagnetically coupled.<sup>25</sup> However, it is clear that the coupling in  $[\text{HB}(\text{pz})_3\text{VO}(\text{OH})_2]_2$  is anomalously low (*i.e.*,  $-40$  vs. *ca.*  $-150(20)$   $\text{cm}^{-1}$ ) compared to that seen in the related complexes.<sup>25</sup> Therefore, based on the magnetic structural correlation presented for the family of binuclear RO-bridging octahedral V(IV)-oxo complexes we could make a prediction about the dihedral angle between the equatorial planes when it is not possible to obtain crystals suitable for X-ray analysis. For example  $[\{\text{VO}(\text{Hhebab})\}_2]$  ( $\text{H}_3\text{hebab}$  = 1,1-bis(2-hydroxyethyl)-4-(2-hydroxybenzyl)-1,4-diazabutane) shows a coupling constant,  $J = -170$   $\text{cm}^{-1}$ ,<sup>25</sup> which corresponds to  $\tau \approx 180^\circ$ , similar to that found in complexes **1** and **4**. This prevision is in agreement with that based on spectroscopic data and functional density calculations.<sup>26</sup>

### Acknowledgements

We acknowledge grants from CAPES-Projeto PROBRAL, CNPQ (PIBIC), DLR (Germany). We thank Professor Dr J. Strähle (Institut für Anorganische Chemie der Universität Tübingen, Germany) for X-ray diffraction facilities.

### References

- 1 V. H. Crawford, H. W. Richardson, J. R. Wasson, D. J. Hodgson and W. E. Hatfield, *Inorg. Chem.*, 1976, **15**, 2107.
- 2 S. M. Gorun and S. J. Lippard, *Inorg. Chem.*, 1991, **30**, 1625.
- 3 A. Niemann, U. Bossek, K. Wieghardt and B. Nuber, *Angew. Chem., Int. Ed. Engl.*, 1992, **31**, 311.

- 4 K. K. Nanda, L. K. Thompson, J. N. Bridson and K. Nag, *J. Chem. Soc., Chem. Commun.*, 1994, 1337.
- 5 W. Plass, *Angew. Chem., Int. Ed. Engl.*, 1996, **35**, 627.
- 6 A. Rawas, H. Muirhead and J. Williams, *Acta Crystallogr., Sect. D*, 1996, **52**, 631.
- 7 E. Sabbioni and E. Marafante, *Bioinorg. Chem.*, 1978, **9**, 389.
- 8 W. R. Harris and C. J. Carrano, *J. Inorg. Biochem.*, 1984, **22**, 201.
- 9 A. Neves, A. S. Ceccato, C. Erasmus-Buhr, S. Gehring, W. Haase, H. Paulus, O. R. Nascimento and A. A. Batista, *J. Chem. Soc., Chem. Commun.*, 1993, **23**, 1782.
- 10 J. Salta, C. J. O'Connor, S. Li and J. Zubieta, *Inorg. Chim. Acta*, 1996, **250**, 303.
- 11 L. Mers and W. Haase, *J. Chem. Soc., Dalton Trans.*, 1980, 875.
- 12 C. J. O'Connor, *Prog. Inorg. Chem.*, 1982, **29**, 203.
- 13 Enraf-Nonius, CAD-4 Express Software, Version 5.0. Enraf-Nonius, Delft, The Netherlands, 1992.
- 14 A. C. T. North, D. C. Phillips and F. S. Mathews, *Acta Crystallogr., Sect. A*, 1968, **24**, 351.
- 15 G. M. Sheldrick, SHELXS97, Program for the Solution of Crystal Structures, University of Göttingen, Germany, 1997.
- 16 G. M. Sheldrick, SHELXL97, Program for the Refinement of Crystal Structures, University of Göttingen, Germany, 1997.
- 17 L. Zsolnai, ZORTEP, An Interactive ORTEP Program, University of Heidelberg, Germany, 1996.
- 18 P. E. Riley, V. L. Pecoraro, C. J. Carrano, J. A. Bonadies and K. N. Raymond, *Inorg. Chem.*, 1986, **25**, 154.
- 19 N. D. Chasteen, *Biological Magnetic Resonance*, ed. L. Berliner and J. Reuben, Plenum, New York, 1981, vol. 3, p. 53.
- 20 A. P. Ginsberg, *Inorg. Chim. Acta Rev.*, 1971, **5**, 45.
- 21 N. D. Chasteen, E. M. Lord, H. J. Thompson and J. K. Grady, *Biochim. Biophys. Acta*, 1986, **884**, 84.
- 22 M. Mikuriya and M. Fukuya, *Bull. Chem. Soc. Jpn.*, 1996, **69**, 679.
- 23 A. Neves and K. Wieghardt, *Inorg. Chim. Acta*, 1988, **150**, 183.
- 24 K. Wieghardt, U. Bossek, K. Volckmar, W. Swiridoff and J. Weiss, *Inorg. Chem.*, 1984, **23**, 1387.
- 25 N. S. Dean, M. R. Bond, C. J. O'Connor and C. J. Carrano, *Inorg. Chem.*, 1996, **35**, 7643.
- 26 W. Plass, *Z. Anorg. Allg. Chem.*, 1997, **623**, 1290.
- 27 WINEPR SIMFONIA version 1.25, Bruker Analytische Messtechnik GmbH, 1996.